Chapter 4

Forward and Adjoint Modeling using Green's Functions

Forward modeling of the wave equation is defined as computing the seismograms for a given source-receiver distribution and a velocity model. This chapter shows how to compute these seismograms using Green's theorem, which casts the solution of the wave equation in terms of a boundary integral and a source-related volume integral. These integral solutions are too costly to compute by the standard boundary integral equation method, so a Lippmann-Schwinger (LS) equation is used under the Born approximation. The LS equation computes the seismograms by a model-coordinate summation of weighted Green's functions, where the weights are the reflection-like coefficients in the model. Another name for this is diffraction-stack modeling. If the adjoint of the Green's function is used (complex conjugate of the Green's function), then the migration image is obtained by a data-coordinate summation of the weighted adjoint Green's functions, where the weights are the seismograms. Another name for this is diffraction-stack migration. These methods are used in later chapters that describe least squares migration and waveform tomography.

The mathematics for the forward modeling equations can be somewhat complicated so that it is easy to lose the physical meaning and motivation for forward modeling. Thus, the next section intuitively derives the equations for convolutional forward modeling of a 1D earth model. Later sections use Green's theorem to generalize these equations to arbitrary media.

4.1 1D Convolutional Modeling

The motivation for modeling waves, i.e., solving the wave equation, is to make a direct connection between geology and the wiggles seen in the recorded seismograms. For example, the sonic and density logs can be used to estimate the 1D layered model of the earth and from these the associated zero-offset (or stacked) seismograms are computed by a forward modeling method. The reflections from a, say, sand-shale interface can be identified in the synthetic trace and correlated to the corresponding event in the recorded stacked sections. Thus, the lithology of each wiggle in the recorded data can be geologically, in principle, identified. This identification will tremendously increase the chances for a correct geological

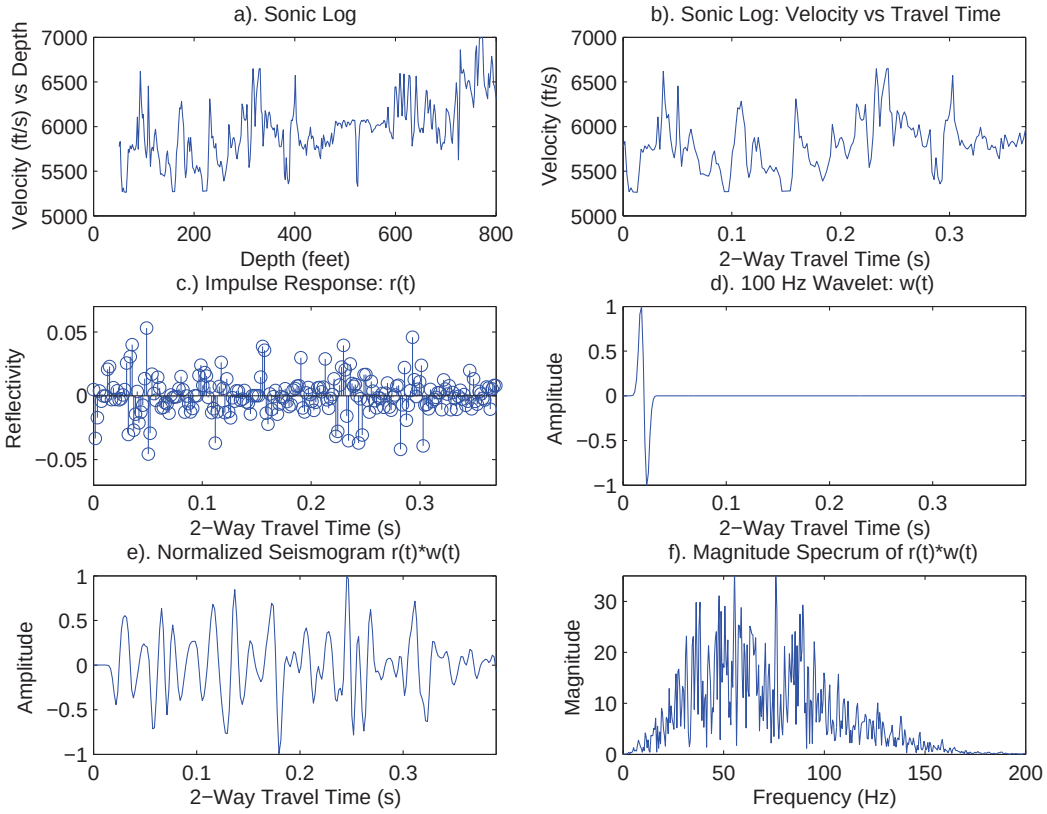

Figure 4.1: a). Sonic log vs depth from Texas, b). sonic log vs 2-way traveltime, c). reflectivity vs time, d). source wavelet vs time, e). normalized seismogram $s(t) = r(t) \star w(t)$, f). magnitude spectrum of seismogram.

interpretation of the seismic traces.

The simplest forward modeling procedure is known as the 1D convolutional model of the earth. In this procedure, a 1D layered model is assumed and parameterized by the density $\rho(z)'$ and velocity $v(z)'$ as a function of depth, as shown in Figure 4.1a. These two functions undergo a depth to 2-way time transformation using the following coordinate transformation:

$$t(z) \quad = \quad 2 \int_0^z dz'/v(z')', \tag{4.1}$$

where $t(z)$ is the 2-way propagation time for energy to go vertically downward from the surface to the horizontal reflector at depth z and back up to the surface in the 1D layered model. A MATLAB script for this mapping from depth to time is given as

```
%%%%%%%%%%%%%%%%%%%%%%%%%%%%
% Finds t(z) from v(z). Assumes
% v(z) starts at free surface.
% v(z)   - input- sonic log as function of z
% dz     - input- depth sampling interval of sonic log
```

```
% t(z)   - input- 2-way time as function of z
%%%%%%%%%%%%%%%%%%%%%%%%%%%%%
function [time]=depth2time(v,dz)
nz=length(v);time=zeros(nz,1); time(1)=dz/v(1);
for i=2:nz; time(i)=time(i-1)+dz/v(i); end
time=time*2; plot(dz*[1:nz],time);
xlabel('Depth (ft)'); ylabel('Time (s)')
title('Depth vs 2-way Time');figure
plot(time,v);xlabel('Time (s)');ylabel('Velocity (ft/s)')
```

The velocity model as a function of time $v(t)$ (see Figure 4.1b) is usually unevenly sampled. To perform convolutional forward modeling, we must convert to an evenly sampled function in time $v(t) = v(t(z))'$; the MATLAB code for getting an even sampled function sampled at the sampling interval dt from an unevenly sampled function is given in Appendix D.

Assuming that the velocity function $v(t)$ is now an evenly sampled function, the evenly sampled zero-offset (ZO) reflection coefficients as a function of time can be estimated by $r(t) = (\rho(t)v(t) - \rho(t-dt)v(t-dt))/((\rho(t)v(t) + \rho(t-dt)v(t-dt))$, which in MATLAB script becomes for constant density:

```
y=diff(vpp);nl=length(y);dt=diff(time);add=vpp(1:nl)+vpp(2:nl+1);
rc=y(1:nl)./add(1:nl);stem(time(1:nl),rc(1:nl));
```

If the density profile is known then the density can be put into the above reflection coefficient formula.

The bandlimited response of the medium for a plane wave input (with source wavelet $w(t)$ as shown in Figure 4.1d) into the surface is a combination of arrivals, including primary and multiple reflections. If attenuation, transmission losses and multiples are excluded then the 1D convolutional model of the seismogram $s(t)$ is given by

$$s(t) = \int_{-\infty}^{\infty} r(\tau)w(t-\tau)d\tau, \tag{4.2}$$

which is the definition of convolution of $r(t)$ with $w(t)$, often abbreviated as $s(t) = r(t) \star w(t)$.

The above formula can be derived by taking the special case of the impulse response where the source wavelet is a Dirac delta function that is excited at time equal to zero: $w(t) = \delta(t)$, where the delta function is defined as $\delta(t) = 0$ if $t \neq 0$, otherwise $\delta(t) = 1$ in the sense $\int \delta(t)dt = 1$. Plugging this impulse wavelet into the above equation yields:

$$\begin{aligned} s(t) &= \int_{-\infty}^{\infty} r(\tau)\delta(t-\tau)d\tau, \\ &= r(t), \end{aligned} \tag{4.3}$$

which describes the reflection coefficient series shown in Figure 4.1c. Thus, the 1D impulse response of the earth under the above assumptions perfectly describes the reflection coefficient series as a function of 2-way traveltime. If the source wavelet were weighted by the scalar weight $w(\tau_i)$ and delayed by time τ_i then $w(t) = w(\tau_i)\delta(t-\tau_i)$ then the delayed impulse response of the earth would be

$$\begin{aligned} s(t)' &= \int_{-\infty}^{\infty} r(\tau)w(\tau_i)\delta(t-\tau_i-\tau)d\tau, \\ &= w(\tau_i)r(t-\tau_i), \end{aligned} \tag{4.4}$$

which is a weighted delayed version of the original impulse response in equation 4.2. If we were to sum these two seismograms we would get, by linearity of integration,

$$s(t)' + s(t) \quad = \quad w(\tau_0)r(t-\tau_0) + w(\tau_i)r(t-\tau_i), \tag{4.5}$$

where $\tau_0 = 0$ and $w(\tau_0) = 1$. By the superposition property of waves (i.e., interfering wave motions add together), we could have performed these two seismic experiments at the same time and the resulting seismograms would be identical mathematically to equation 4.5. More generally, the earth's resposne to an arbitrary wavelet $w(\tau)$ is given by

$$\begin{aligned} s(t) &= \sum_i w(\tau_i)r(t-\tau_i), \\ &\approx \int_{-\infty}^{\infty} w(\tau)r(t-\tau)d\tau, \end{aligned} \tag{4.6}$$

and in the limit of vanishing sampling interval dt the approximation becomes an equality (see Figure 4.1e). Under the transformation of variables $\tau' = t - \tau$ equation 4.6 becomes

$$s(t) \quad = \quad \int_{-\infty}^{\infty} w(t-\tau')r(\tau')d\tau', \tag{4.7}$$

which is precisely the convolution equation shown in equation 4.2. The equality of equations 4.6 and 4.7 also shows that convolution commutes, i.e., $s(t) = r(t) \star w(t) = w(t) \star r(t)$. The convolutional modeling equation was practically used by many oil companies starting in the 1950's, and is still in use today for correlation of well logs to surface seismic data.

4.1.1 Multiples

Multiples associated with a strong reflector and the free surface can be accounted for in the 1D modeling equations. For a sea-bottom with depth d and two-way ZO traveltime τ_w, the sea-bed impulse response for ZO downgoing pressure waves a source and pressure receiver just below the sea surface is given by

$$m(t) \quad = \quad w(t) + \sum_{i=1}^{\infty} (-R)^i w(t - i\tau_w) \tag{4.8}$$

where R is the ZO reflection coefficient of the sea floor; the -1 accounts for the free surface reversal of polarity and $w(t)$ is the source wavelet of the airgun modified by the interaction with the sea-surface reflectivity. We assume that the propagation time between the surface and hydrophone streamer is negligible compared to the propagation time from the surface to the sea floor. as illustated in Figure 4.2a.

The upgoing multiples each act as a secondary source on the sea surface, so we can consider the "generalized" source wavelet to be $m(t)$. Thus the response of the medium is given by

$$s(t) \quad = \quad r(t) \star m(t). \tag{4.9}$$

These multiples tend to blur the reflectivity response so we should try to deconvolve the multiples.

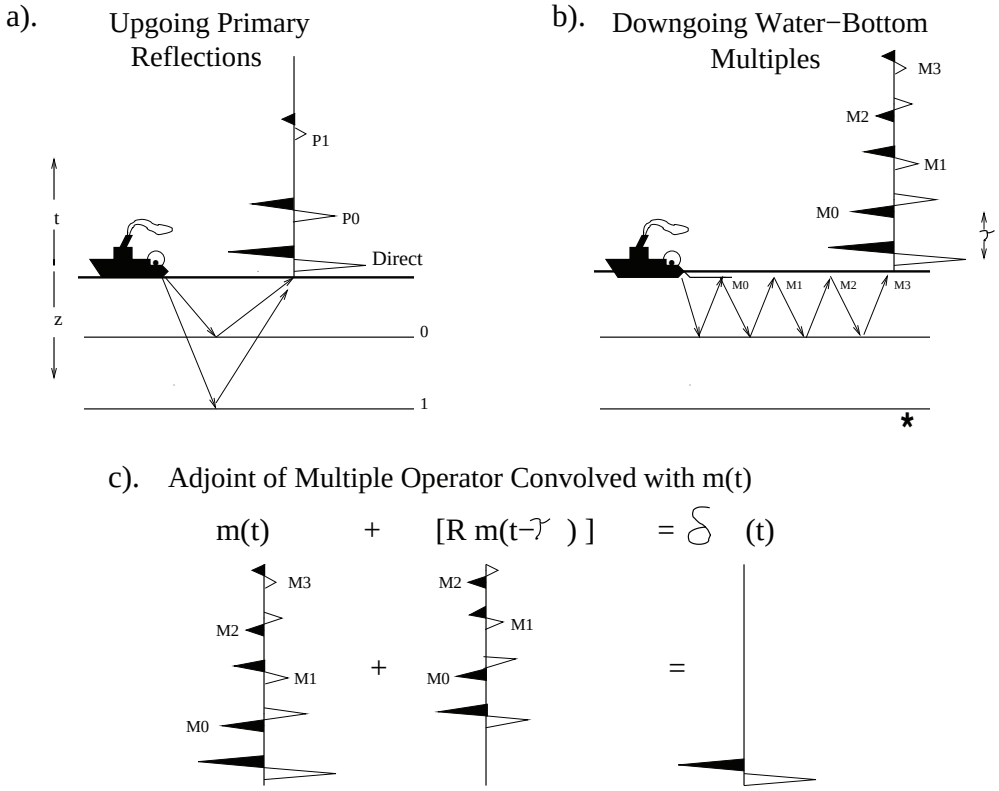

Figure 4.2: a). Upgoing primary reflections, b). downgoing sea-floor multiples only and c). adjoint of multiple operator applied to multiples to give a quasi-spike at $t = 0$. Here, vertical incidence angles are assumed in a layer-cake model and the wavelet in c). is a delta function.

The "deblurring" or deconvolution operator can be found in the frequency domain by taking the Fourier transform of equation 4.8:

$$\begin{aligned} M(\mathbf{Z}) &= W(\mathbf{Z})(1+\sum_{i=1}^{\infty}(-R)^i\mathbf{Z}^{i\tau_w}), \\ &= \frac{W(\mathbf{Z})}{1+R\mathbf{Z}^{\tau_w}}, \end{aligned} \tag{4.10}$$

where $\mathbf{Z} = e^{-j\omega}$. Thus, the free-surface demultiple operator for downgoing waves in equation 4.9 is given in the frequency domain by

$$\begin{aligned} M(\mathbf{Z})^{-1} &= (1+R\mathbf{Z}^{\tau_w})/W(\mathbf{Z}), \\ &= (1+R\mathbf{Z}^{\tau_w})W(\mathbf{Z})^*/|W(\mathbf{Z})|^2, \end{aligned} \tag{4.11}$$

or in the time domain as

$$m(t)^{-1} = (1+R\delta(t-\tau_w)) * w(t)^{-1}. \tag{4.12}$$

as illustrated in Figure **??**c. The deblurring operator says that the seismogram must be added to a weighted-delayed copy of itself, where the weighting is R and the delay is the two-way propagation time through the water layer. In addition, the wavelet inverse must be convolved with this result.

4.2 1D Adjoint Convolutional Modeling

The adjoint operator is sometimes a good approximation to the inverse operator, as explained in the previous chapter. For equation 4.7, the inverse can be approximated by applying the adjoint operator $\int_{-\infty}^{\infty} w(t+t')dt$ to $s(t)$, i.e.,

$$r(\tau) \approx \int_{-\infty}^{\infty} w(\tau+t)s(t)dt. \tag{4.13}$$

This can be seen to be a good approximation by substituting $s(t) = \int_{-\infty}^{\infty} r(\tau')w(t-\tau')d\tau'$ to give

$$\begin{aligned} r(\tau) &\approx \int_{-\infty}^{\infty}[\int_{-\infty}^{\infty} w(t-\tau')w(\tau+t)dt]r(\tau')d\tau', \\ &= \int_{-\infty}^{\infty}\phi_{ww}(\tau-\tau')r(\tau')d\tau', \\ &\approx r(\tau). \end{aligned} \tag{4.14}$$

where the approximation follows if the wavelet is a vibroseis chirp over a wideband of frequencies so that $\phi_{ww}(\tau-\tau') \approx \delta(\tau-\tau')$. In this case we say that $\int_{-\infty}^{\infty} w(t-t')dt$ is an approximate inverse operator or we can say it is the adjoint modeling operator.

4.2.1 1D Adjoint for Multiples

The inverse to the free-surface multiple operator in equation 4.10 can be approximated by its adjoint operator

$$\begin{aligned} M(\mathbf{Z})^{-1} &\approx \frac{W(\mathbf{Z})^*}{1+R\mathbf{Z}^{-\tau_w}}, \\ &= \frac{W(\mathbf{Z})^*(1+R\mathbf{Z}^{\tau_w})}{|1+R\mathbf{Z}^{-\tau_w}|^2}, \end{aligned} \tag{4.15}$$

which has exactly the same phase spectrum as the actual inverse in equation 4.11. Their magnitude spectrums only differ by the absence of the $|W(\mathbf{Z})|^2$ in the denominator of equation **??** and the inclusion of the $|1+R\mathbf{Z}^{-\tau_w}|^2$ term. These terms can be harmlessly ignored if they have a constant value over the frequency band of the signal.

.

4.3 3D Integral Equation Forward Modeling

The previous section assumed no geomteric spreading losses, no multiples, a layered media and no transmission losses. These assumptions are unrealistic for many purposes, so we must learn how to solve the wave equation for arbitrary acoustic media using Green's theorem. Extensions to anelastic media are straightforward.

The 3D Helmholtz equation is given by

$$(\nabla^2_{\mathbf{r}'} + \omega^2 s(\mathbf{r}')^2)\tilde{P}(\mathbf{r}') = \tilde{F}(\mathbf{r}'), \tag{4.16}$$

where the wavenumber $k = \omega/c(\mathbf{r})$ is for an inhomogeneous medium with velocity $c(\mathbf{r})$, $\tilde{F}(\mathbf{r})$ is the source term associated with a harmonically oscillating source at $\mathbf{r}$, and $\tilde{P}(\mathbf{r}')$ is the associated pressure field.

The goal of forward modeling is, given the source-receiver coordinates and the velocity model, use Green's theorem to find the pressure field in the form of an integral equation. Towards this goal, we first define a Green's function and then use it to derive Green's theorem.

4.3.1 Green's Functions

The Green's function associated with the 3-D Helmholtz equation for an arbitrary medium (Morse and Feshback, 1953) solves

$$(\nabla^2_{\mathbf{r}'} + k^2)\tilde{G}(\mathbf{r}'|\mathbf{r}) = \delta(\mathbf{r}'-\mathbf{r}), \tag{4.17}$$

where $k = \omega/c(\mathbf{r})$ and $\delta(\mathbf{r}'-\mathbf{r}) = \delta(x-x')\delta(y-y')\delta(z-z')$.

There are two independent solutions to this 2nd-order PDE: an outgoing Greens function $\tilde{G}(\mathbf{r}|\mathbf{r}')$ and its complex conjugate the incoming Green's function $\tilde{G}(\mathbf{r}|\mathbf{r}')^*$. The outgoing Green's function (see Appendices A and B) for a homogeneous medium with velocity c_0 is given by

$$\tilde{G}(\mathbf{r}|\mathbf{r}') = -\frac{1}{4\pi}e^{-ik_0|\mathbf{r}'-\mathbf{r}|}/|\mathbf{r}-\mathbf{r}'|, \tag{4.18}$$

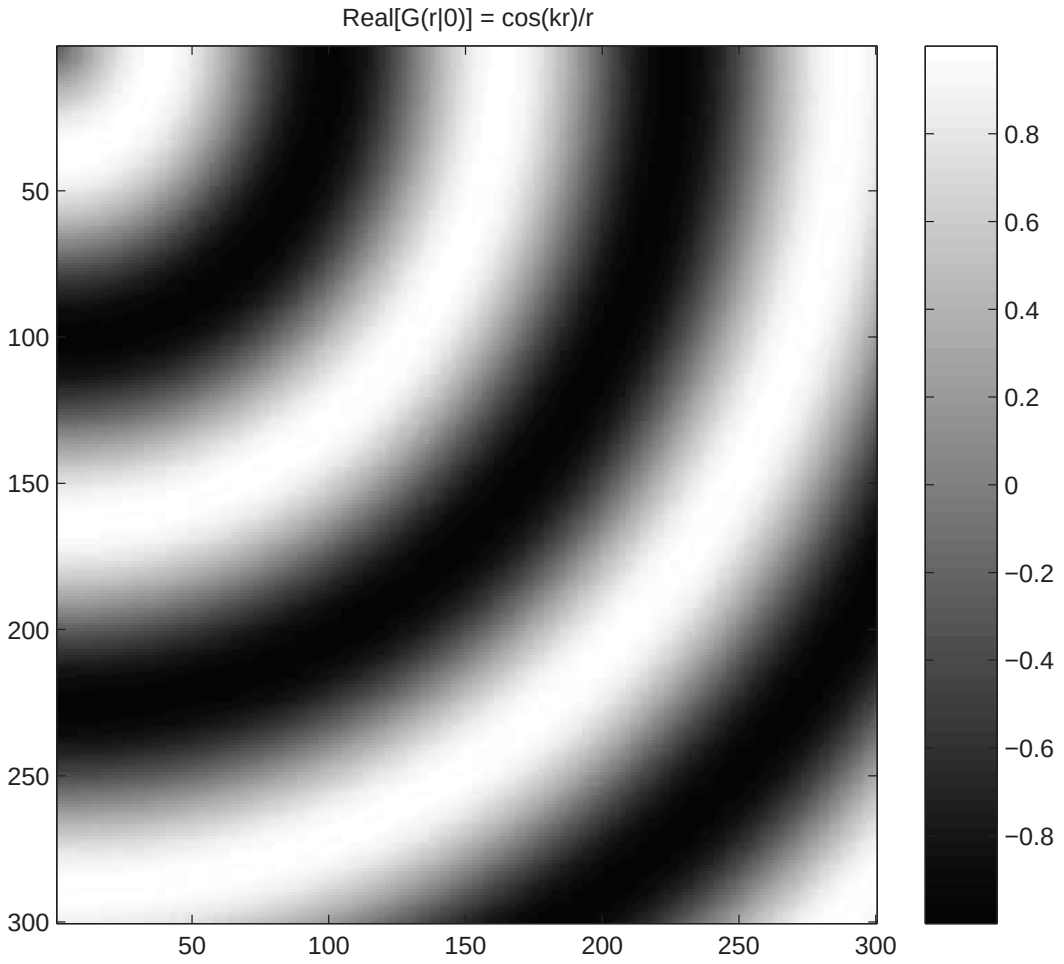

Figure 4.3: Snapshot of the real part of the harmonic Green's function, where the geometrical spreading factor has been ignored.

where the wavenumber is given by $k_0 = \omega/c_0$, the denominator represents the geometrical spreading factor while the exponential phase factor is proportional to the with distance between the observer $\mathbf{r}$ and the source point $\mathbf{r}'$. The interpretation of the Green's function is that it is the acoustic response measured at $\mathbf{r}$ for a harmonically oscillating point source located at $\mathbf{r}'$.

For a homogeneous medium the Green's function plots out as a series of concentric circles centered about $\mathbf{r}'$ with wavelength $\lambda_o = 2\pi c_o/\omega$ (see Figure 4.3). Note, the source and receiver locations can be interchanged in equation 4.18 so that $\tilde{G}(\mathbf{r}|\mathbf{r}') = \tilde{G}(\mathbf{r}'|\mathbf{r})$, which is the reciprocity principle. This says that a trace recorded at position A excited by a source at B will be the same as the trace located at B for a source excitation at A.

4.3.2 $(\nabla^2_{\mathbf{r}'} + k^2)^{-1}$ by Green's theorem

Green's theorem will be used to invert equation 4.16. Multiplying the Helmholtz equation by the Green's function gives

$$\tilde{G}(\mathbf{r}|\mathbf{r}')(\nabla^2_{\mathbf{r}'} + k^2)\tilde{P}(\mathbf{r}') = \tilde{G}(\mathbf{r}|\mathbf{r}')\tilde{F}(\mathbf{r}'), \tag{4.19}$$

where the differentiation in $\nabla_{\mathbf{r}'}$ is with respect to the primed coordinates. Inserting the identity $\tilde{G}\nabla^2_{\mathbf{r}'}\tilde{P} = \tilde{P}\nabla^2_{\mathbf{r}'}\tilde{G} + \nabla_{\mathbf{r}'}\cdot(\tilde{G}\nabla_{\mathbf{r}'}\tilde{P} - \tilde{P}\nabla_{\mathbf{r}'}\tilde{G})$ (which can be proved using differentiation by parts) into the above equation gives

$$\tilde{P}(\mathbf{r}')(\nabla^2_{\mathbf{r}'} + k^2)\tilde{G}(\mathbf{r}|\mathbf{r}') + \nabla_{\mathbf{r}'}\cdot(\tilde{G}\nabla_{\mathbf{r}'}\tilde{P} - \tilde{P}\nabla_{\mathbf{r}'}\tilde{G}) = \tilde{G}(\mathbf{r}|\mathbf{r}')\tilde{F}(\mathbf{r}'). \tag{4.20}$$

Integrating equation 4.20 over the entire model volume yields

$$\int_{vol}[\tilde{P}(\mathbf{r}')(\nabla^2_{\mathbf{r}'} + k^2)\tilde{G}(\mathbf{r}|\mathbf{r}') + \nabla_{\mathbf{r}'}\cdot(\tilde{G}\nabla_{\mathbf{r}'}\tilde{P} - \tilde{P}\nabla_{\mathbf{r}'}\tilde{G})]dV' = \int_{vol}\tilde{G}(\mathbf{r}|\mathbf{r}')\tilde{F}(\mathbf{r}')dV' \tag{4.21}$$

and inserting equation 4.17 yields

$$\int_{vol}\tilde{P}(\mathbf{r}')\delta(\mathbf{r}' - \mathbf{r})dV' + \int_{vol}\nabla_{\mathbf{r}'}\cdot(\tilde{G}\nabla_{\mathbf{r}'}\tilde{P} - \tilde{P}\nabla_{\mathbf{r}'}\tilde{G})dV' = \int_{vol}\tilde{G}(\mathbf{r}|\mathbf{r}')\tilde{F}(\mathbf{r}')dV', \tag{4.22}$$

or

$$\tilde{P}(\mathbf{r}) + \int_{surf}(\tilde{G}\nabla_{\mathbf{r}'}\tilde{P} - \tilde{P}\nabla_{\mathbf{r}'}\tilde{G})\cdot d\vec{A}', = \int_{vol}\tilde{G}(\mathbf{r}|\mathbf{r}')\tilde{F}(\mathbf{r}')dV', \tag{4.23}$$

where the unit normal is pointing outward from the body. The conversion from a volume integral to a surface integral follows by the divergence theorem (Morse and Feshbach, 1953; Barton, 1989). Rearranging gives the integral equation solution to the Helmholtz equation:

$$\tilde{P}(\mathbf{r}) = -\int_{surf}(\tilde{G}\nabla_{\mathbf{r}'}\tilde{P} - \tilde{P}\nabla_{\mathbf{r}'}\tilde{G})\cdot d\vec{A}' + \int_{vol}\tilde{G}(\mathbf{r}|\mathbf{r}')F(\mathbf{r}')dV'. \tag{4.24}$$

The above integral is the starting point for the Boundary Integral Equation modeling method (Brebbia, 1978; Schuster, 1985 and many others).

If only outgoing waves are considered and the surface integral is at infinity then the surface integration is zero in equation 4.25 to give

$$\tilde{P}(\mathbf{r}) = \int_{vol}\tilde{G}(\mathbf{r}|\mathbf{r}')F(\mathbf{r}')dV'. \tag{4.25}$$

The physical interpretation of this term is that it represents the direct wave. Therefore, the boundary integral in equation 4.24 represents the boundary reflections and echoes that contribute to the field inside the volume.

This solution of the Helmholtz equation given by equation 4.25 is a weighted sum of the Green's functions, where the weights are the source amplitudes at each point in the medium. This representation is valid for an arbitrary acoustic medium, and shows that $\int dV'\tilde{G}(\mathbf{r}|\mathbf{r}')\cdot = (\nabla^2_{\mathbf{r}'} + k^2)^{-1}$. In other words, applying the *appropriate* Green's function to the Helmholtz equation and integrating over the volume is the inverse operator to the Helmholtz equation.

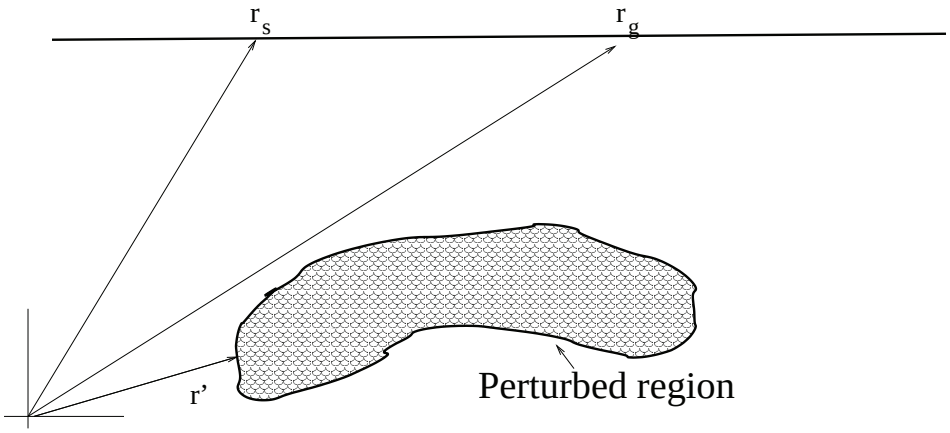

Figure 4.4: Background medium with an embedded potato-like perturbation of slightly different velcoity.

4.3.3 Lippmann-Schwinger Solution

Equation 4.24 is expensive to solve for the unknown field values $\tilde{P}(\mathbf{r})$ because they are on both the left and right hand sides, which means an expensive matrix inverse (Schuster, 1985) must be computed. To avoid this expense we use the Lippmann-Schwinger equation under the Born approximation, as described below.

Assume a medium composed of the background slowness and a perturbed slowness given by $s(\mathbf{r}) + \delta s(\mathbf{r})$, where $\delta s(\mathbf{r})$ is sufficiently small. For example, Figure 4.4 shows the background medium as homogeneous and the perturbed region as potato-shaped with a slightly different velocity.

The pressure field $\tilde{P}$ in the perturbed medium is governed by

$$(\nabla^2_{\mathbf{r}'} + \omega^2[s(\mathbf{r}') + \delta s(\mathbf{r}')]^2)\tilde{P}(\mathbf{r}') \quad = \quad \tilde{F}(\mathbf{r}'), \tag{4.26}$$

or by rearranging we get

$$(\nabla^2_{\mathbf{r}'} + \omega^2 s(\mathbf{r}')^2)\tilde{P}(\mathbf{r}') \quad = \quad -2\omega^2 s(\mathbf{r}')\delta s(\mathbf{r}')\tilde{P}(\mathbf{r}') + \tilde{F}(\mathbf{r}'), \tag{4.27}$$

where second-order terms in the perturbation parameter are neglected. The above Helmholtz equation can be inverted by applying $\int dV' \tilde{G}(\mathbf{r}|\mathbf{r}')\cdot$ to both sides of the above equation to

give the Lippmann-Schwinger equation:

$$\tilde{P}(\mathbf{r}) = -2\omega^2 \int_{vol} \overbrace{\tilde{G}(\mathbf{r}|\mathbf{r}')}^{Upgoing\ field} \overbrace{s(\mathbf{r}')\delta s(\mathbf{r}')}^{Reflectivity} \overbrace{\tilde{P}(\mathbf{r}')}^{Downgoing\ field} dV' + \int_{vol} \tilde{G}(\mathbf{r}|\mathbf{r}')\tilde{F}(\mathbf{r}')dV', \tag{4.28}$$

where the Green's function is that for the unperturbed medium and satisfies equation 4.17 for $k = \omega s(x)$. The term $\tilde{P}(\mathbf{r}')$ represents the total field on the potato exited from an overlying source distribution so we call this the *downgoing field*. Similarly, the Green's function $\tilde{G}(\mathbf{r}|\mathbf{r}')$ takes the incident field on the potato and extrapolates it to the surface as an *upgoing field*; the strength of this upgoing field is proportional to the magnitude of the $reflectivity - like$ term $s(\mathbf{r}')\delta s(\mathbf{r}')$.

Note, the unknown field value $\tilde{P}(\mathbf{r}')$ is on both the left and right hand side of equation 4.28; this means that this unknown can be determined by discretizing the field values, the slowness distribution and replacing the integral by a numerical quadrature to give a large system of integral equations, similar to the boundary integral equation method (Brebbia, 1978).

4.3.4 Neumann Series Solution

An alternative to the direct inversion of this system of equations is an iterative solution, such as the Neummann series solution to equation 4.28. A Neumann series solution is similar to the scalar geometric series

$$(1-x)^{-1} = 1 + x + x^2 + x^3 + ... \tag{4.29}$$

that converges for $||x|| < 1$, except x represents an operator. Rearranging equation 4.28 so that the terms in the unknown $\tilde{P}(\mathbf{r}')$ equation 4.28 are on the lefthand side gives

$$[\int_{vol} \delta(\mathbf{r}' - \mathbf{r})dV' + 2\omega^2 \int_{vol} \tilde{G}(\mathbf{r}|\mathbf{r}')s(\mathbf{r}')\delta s(\mathbf{r}')dV']\tilde{P}(\mathbf{r}') = \int_{vol} \tilde{G}(\mathbf{r}|\mathbf{r}')\tilde{F}(\mathbf{r}')dV', \tag{4.30}$$

so that the operator x in the Neumann series here is identified as

$$x \rightarrow -2\omega^2 \int_{vol} \tilde{G}(\mathbf{r}|\mathbf{r}')s(\mathbf{r}')\delta s(\mathbf{r}')dV'. \tag{4.31}$$

Therefore, the Neumann series solution to equation 4.28 is

$$\tilde{P}(\mathbf{r}) = \int_{vol} \overbrace{\tilde{G}(\mathbf{r}|\mathbf{r}')\tilde{F}}^{\psi_0}(\mathbf{r}')dV' - 2\omega^2 \int_{vol} \overbrace{\tilde{G}(\mathbf{r}|\mathbf{r}')s(\mathbf{r}')\delta s(\mathbf{r}') \int_{vol} \tilde{G}(\mathbf{r}'|\mathbf{r}'')\tilde{F}(\mathbf{r}'')\, dV'}^{\mathcal{G}_0 V \psi_0} dV'' +$$

$$4\omega^4 \int_{vol} \overbrace{\tilde{G}(\mathbf{r}|\mathbf{r}')s(\mathbf{r}')\delta s(\mathbf{r}') \int_{vol} \tilde{G}(\mathbf{r}'|\mathbf{r}'')s(\mathbf{r}'')\delta s(\mathbf{r}'') \int_{vol} \tilde{G}(\mathbf{r}''|\mathbf{r}''')\tilde{F}(\mathbf{r}''')}^{\mathcal{G}_0 V \mathcal{G}_0 V \psi_0} dV' dV'' dV''' + ...$$

$$= \int_{vol} \tilde{G}(\mathbf{r}|\mathbf{r}')\tilde{F}(\mathbf{r}')dV' + \sum_{i=1}^{\infty} [-2\omega^2 \int_{vol} \tilde{G}(\mathbf{r}|\mathbf{r}')s(\mathbf{r}')\delta s(\mathbf{r}')dV']^i \int_{vol} \tilde{G}(\mathbf{r}'|\mathbf{r}'')\tilde{F}(\mathbf{r}'')dV'';$$

or in more compact notation we can represent the above equation by

$$P = \sum_{i=0}^{\infty} [\mathcal{G}_0 V]^i \psi_0 = P^{(0)} + P^{(1)} + P^{(2)} + ... , \tag{4.32}$$

where the *nth* term represents the *nth* order response of the perturbed medium. For example, the zeroth-order term $P^{(0)} = \int_{vol} \tilde{G}(\mathbf{r}|\mathbf{r}')\tilde{F}(\mathbf{r}')dV'$ is the direct-wave response of the background medium, the first-order term $P^{(1)}$ is the primary $reflection$ response between the *potato* and the background medium, the second-order term $P^{(2)}$ is its 1st-order multiple response, and so on. The first-order term $P^{(1)}$ is also known as the Born approximation, as discussed in the next section.

4.3.5 Born Approximation

The Born approximation is nothing more than approximating the scattered field $P - P_0$ by the first-order term of the Born series in equation 4.36:

$$P - P^{(0)} \approx P^{(1)}. \tag{4.33}$$

The physical meaning of this approximation is now gievn.

If the perturbed field is "close" to that of the unperturbed field and if the actual source is a point source located at $\mathbf{r}_s$, then $\tilde{P}(\mathbf{r}')$ on the RHS of equation 4.28 can be replaced by $\tilde{G}(\mathbf{r}'|\mathbf{r}_s)W(\omega)$ (where $W(\omega)$ is the source spectrum) to give the Born approximation to the Lippmann-Schwinger equation:

$$\begin{aligned} \tilde{P}(\mathbf{r}|\mathbf{r_s}) &= -2\omega^2 \int_{vol} \tilde{G}(\mathbf{r}|\mathbf{r}')dV's(\mathbf{r}')\delta s(\mathbf{r}')\tilde{W}(\omega)\tilde{G}(\mathbf{r}'|\mathbf{r_s}) \\ &\quad + \int_{vol} \tilde{G}(\mathbf{r}|\mathbf{r}')\tilde{F}(\mathbf{r}')dV', \end{aligned} \tag{4.34}$$

where the first term on the RHS accounts for the primary reflection from the perturbation and the second term accounts for the direct wave in the unperturbed medium. The approximation is valid if multiples inspired by δs can be neglected.

Example of Non-Zero Offset Modeling: We will now derive the diffraction stack modeling equation for a smoothly varying velocity model at high source frequencies, and for a non-zero offset (ZO) configuration where each source shoots into receivers with finite offset.

Assume high frequencies so that the asymptotic Green's function (Bleistein, 1984) can be used:

$$\tilde{G}(\mathbf{r}|\mathbf{r_s}) = \frac{e^{-i\omega\tau_{sr}}}{r}, \tag{4.35}$$

where τ_{sr} is the time for energy to propagate from the source at $\mathbf{r_s}$ to the interrogation point at $\mathbf{r}$, and $1/r_{sr} = 1/|\mathbf{r} - \mathbf{r_s}|$ is the geometrical spreading term that approximates the solution to the transport equation. For convenience we will ignore the $-1/4\pi$ factor.

Substituting equation 4.35 into equation 4.34 we get the diffraction stack equation of forward modeling:

$$\tilde{P}(\mathbf{r}|\mathbf{r_s})^{scatt} = -2\omega^2 \int_{vol} s(\mathbf{r}')\delta s(\mathbf{r}')\tilde{W}(\omega)e^{-i\omega(\tau_{sr'}+\tau_{rr'})}/(|\mathbf{r}' - \mathbf{r_s}||\mathbf{r} - \mathbf{r}'|)dV', \tag{4.36}$$

where the direct wave is neglected to give the scattered field $\tilde{P}(\mathbf{r}|\mathbf{r_s})^{scatt}$. Applying an inverse Fourier transform $\int d\omega e^{i\omega t}$ to the above equation yields the time-domain diffraction stack modeling formula:

$$p(\mathbf{r}, t|\mathbf{r_s}, 0)^{scatt} = -2 \int_{vol} s(\mathbf{r}')\delta s(\mathbf{r}')\ddot{w}(t - \tau_{sr'} - \tau_{rr'})/(|\mathbf{r}' - \mathbf{r_s}||\mathbf{r} - \mathbf{r}'|)dV'. \tag{4.37}$$

This formula can be used to generate synthetic seismograms of primary reflections by setting $\delta s(\mathbf{r}) = 1$ along reflector boundaries, otherwise $\delta s(\mathbf{r}) = 0$.

A special case is for a point scatterer $\delta s(\mathbf{r}) = \delta(\mathbf{r} - \mathbf{r}_0)$ and a geophone at $\mathbf{r} \to \mathbf{r}_g$ so that equation 4.37 becomes

$$p(\mathbf{r}_g, t|\mathbf{r_s}, 0)^{scatt} = -2s(\mathbf{r}_0)\delta s(\mathbf{r}_0)\ddot{w}(t - \tau_{sr_0} - \tau_{gr_0})/(|\mathbf{r}_0 - \mathbf{r_s}||\mathbf{r}_g - \mathbf{r}_0|). \tag{4.38}$$

Here, $w(t)$ describes the time history of the source wavelet, and $w(t - \tau_{sr_0} - \tau_{gr_0})$ is the source wavelet delayed by the amount of time it takes to go from the source down to the scatterer and up to the receiver. The support of $w(t-\tau_{sr_0}-\tau_{gr_0})$ exists along the hyperbola shown in Figure 4.6 because $t = \tau_{sr_0} + \tau_{gr_0} = [\sqrt{(x_0 - x_s)^2 + {z_0}^2} + \sqrt{(x_g - x_0)^2 + {z_0}^2}]/c$ traces out a hyperbola in data-space coordinates $(x_g, 0, t)$. Thus the point scatterer response is obtained by smearing the reflectivity $\delta s(\mathbf{r})$ amplitude along the appropriate hyperbola in data space.

For a string of contiguous point scatterers the seismograms are obtained by *smearing* and *summing* the perturbation amplitudes along the appropriate hyperbolas, one for each scatterer as shown in Figure 4.5.

Example of Zero-Offset Modeling: We will now derive the diffraction stack modeling equation for a zero-offset (ZO) configuration, where each source shoots into only the receiver located at the source point. Recall, after nomral moveout correction of common midpoint gathers and stacking, the resulting section is somewhat equivalent to a ZO section.

When the source is coincident with the geophone then $\tau_{s\mathbf{r}} = \tau_{g\mathbf{r}}$ and equation 4.38 becomes

$$p(\mathbf{r}_s, t|\mathbf{r_s}, 0)^{scatt} = -2s(\mathbf{r}_0)\delta s(\mathbf{r}_0)\ddot{w}(t - 2\tau_{sr_0})/|\mathbf{r}_0 - \mathbf{r_s}|^2. \tag{4.39}$$

In this case the data are smeared along the hyperbola with an apex at the source coordinate.

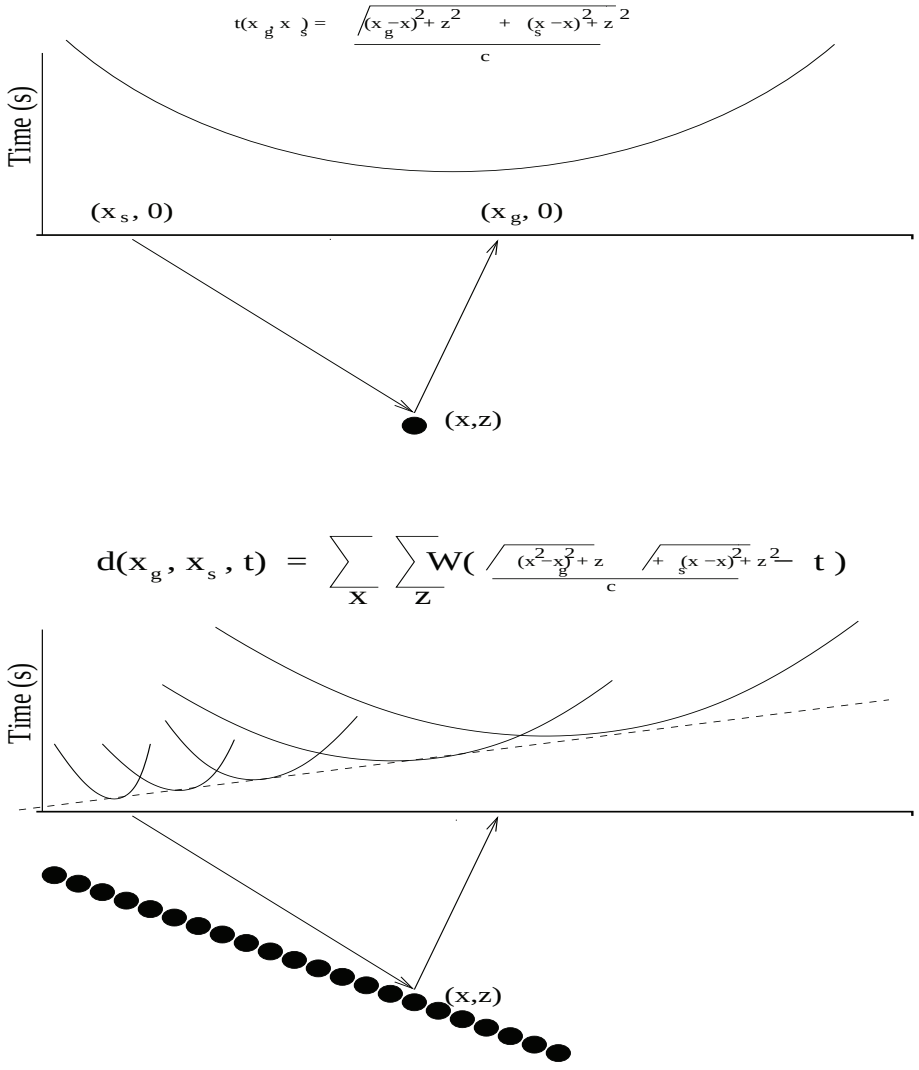

Figure 4.5: Shot gather of traces for a (top) point scatterer and a (bottom) dipping reflector. Bottom formula is that for Born forward modeling, except geometric spreading effects have been neglected. Each reflectivity point is mapped (i.e., smeared) from the model space point (x, z) into the data space as a shifted weighted wavelet, and these events falls along a hyperbola and summed to give the shot gather traces.

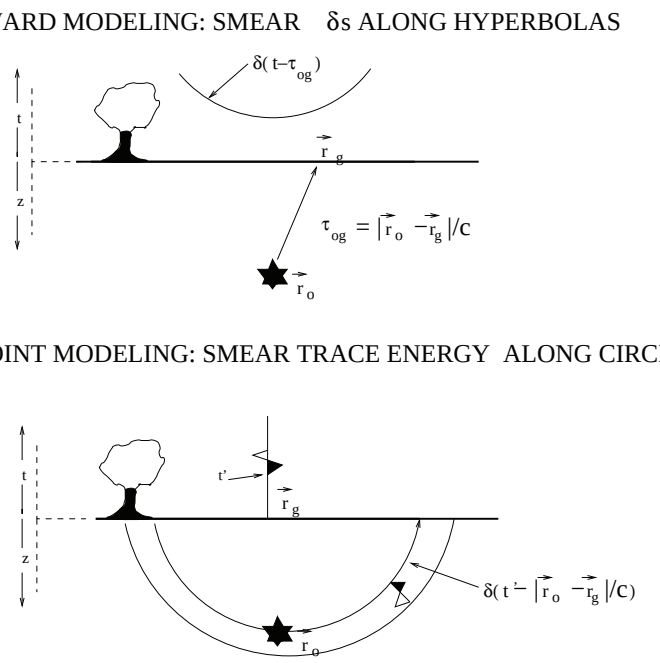

Figure 4.6: (Top) Forward modeling of a point scatterer consists of smearing reflectivity energy along the appropriate hyperbola in data space, and (bottom) adjoint modeling consists of smearing reflection energy in an impulsive trace along the appropriate circle in model space. Zero-offset traces are assumed where the source is coincident with the receiver.

More generally, a model with an interface can be approximated by a sequence of contiguous point scatterers, so that the data are given by the summed contribution of all the point scatterers, i.e.,

$$\begin{aligned} p(\mathbf{r}_s, t|\mathbf{r_s}, 0)^{scatt} &= \sum_x \sum_z r(x,z)\ddot{w}(t = 2\sqrt{(x-x_s)^2 + z^2}/c)/A \\ & where \\ A(x,z,x_s,x_s) &= ||\mathbf{x_s} - \mathbf{x}||^2. \end{aligned} \tag{4.40}$$

This formula includes primary reflections, but excludes multiples and angle-dependent reflection coefficients. It is known as the Born modeling formula, and can be described as smearing+summing the reflectivity values $r(x,z)$ along the appropriate hyperbolas in data space. For an inhomogeneous medium, ray tracing can be used to compute a traveltime table that replaces the square root expression in equation 4.40.

The MATLAB code for zero-offset (i.e., the source position is the same as the receiver position) diffraction stack modeling is given below. The top of Figure 4.7 depicts a zero-offset seismic section generated by this code.

```
% ZERO-OFFSET DIFFRACTION STACK FORWARD MODELING
```

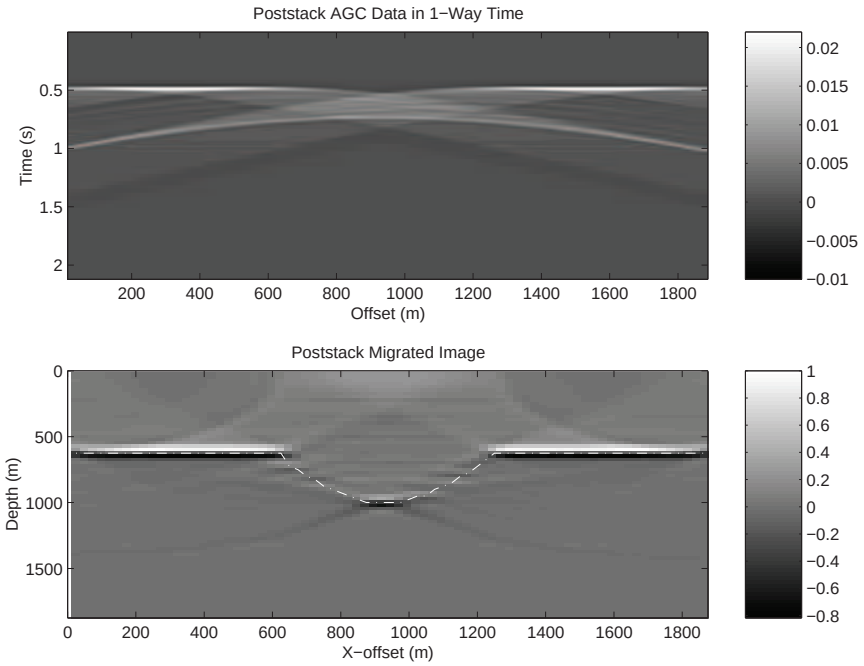

Figure 4.7: (Top) Poststack seismograms and (bottom) migration section generated by diffraction stack forward modeling and adjoint modeling codes, respectively. The model consisted of 75 contiguous point scatterers that defined the synclinal reflector denoted by white dashes in the bottom figure.

```
%
for ixtrace=1:ntrace; %LOOP OVER ALL TRACES
    for ix=1:nx;     %LOOP OVER ALL X-Coord IN MODEL
    for iz=2:nz;     %LOOP OVER ALL Z-Coord IN MODEL
      r = sqrt((ixtrace*dx-ix*dx)^2+(iz*dz)^2); DISTANCE
      time = 1 + round( r/c/dt ); PROPAGATION TIME
      data(ixtrace,time) = mig(ix,iz)/r + data(ixtrace,time);
    end;
    end;
 data1(ixtrace,:)=conv2(data(ixtrace,:),rick)% CONVOLVE
                              % TRACES WITH BANDED WAVELET
                              % rick
end;
```

4.3.6 Matrix Operator Notation

Equation 4.37 gives the integral representation for Born forward modeling. We will now discretize the scattered pressure field, slowness model and modeling operator.

If the slowness field is discretized onto a mesh of N square cells with a constant slowness perturbation Δs_i in the ith cell, equation 4.37 reduces to a linear system of equations for the high-frequency approximation:

$$p_i^{scatt} = \sum_{j=1}^{N} l_{ij} \Delta s_j, \tag{4.41}$$

for $i = 1, .., M$ and

$$l_{ij} \leftrightarrow l_{rst,j} \approx 2\delta(t - \tau_{jr} - \tau_{js}) \frac{dx^2}{|\mathbf{r}_j - \mathbf{r}_r||\mathbf{r}_j - \mathbf{r}_s|}, \tag{4.42}$$

$$p_i^{scatt} \leftrightarrow p_{rst} = p(\mathbf{r}, t|\mathbf{r}_s, 0) \ . \tag{4.43}$$

Here dx is the width of a cell; $i \leftrightarrow (r, s, t)$ denotes the 1-1 mapping between the single data index i and the 3-tuple of data indices (r, s, t); and r, s, and t correspond to the integer indices associated with discretizing the receiver locations $\mathbf{r}$, source locations $\mathbf{r}_s$ and time values t, respectively. Here, the model indices are denoted by j. More compactly, the above system of equations can be represented by

$$\mathbf{L}\ \Delta\mathbf{s} \quad = \quad \mathbf{p^{scatt}}, \tag{4.44}$$

where $\mathbf{L}$ represents the MxN matrix with components l_{ij}, $\mathbf{p^{scatt}}$ is the $Mx1$ vector of pressure data, and $\Delta\mathbf{s}$ is the $Nx1$ vector of slowness perturbations. Note, in the above MATLAB script the $\mathbf{L}$ matrix is not explicitly formed, rather, each trace is computed by the summation indicated in equation 4.41.

4.4 3D Integral Equation Adjoint Modeling

In a later chapter, we will see that the least squares formalism solves for $\mathbf{m}$ in equation 4.44 by using the inverse to the normal equations:

$$\mathbf{m} \quad = \quad [\mathbf{L}^{*\mathbf{T}}\mathbf{L}]^{-\mathbf{1}}\mathbf{L}^{*\mathbf{T}}\mathbf{p} \approx \mathbf{L}^{*\mathbf{T}}\mathbf{p}. \tag{4.45}$$

The estimate for the reflectivity model $\mathbf{m}$ approximated by $\mathbf{L}^{*\mathbf{T}}\mathbf{p}$ is known as the migration image, where $\mathbf{L}^{*\mathbf{T}}$ is the transposed conjugate of $\mathbf{L}$ othrewise known as the adjoint of $\mathbf{L}$.

Adjoint Matrix and Kernel. If the elements of $\mathbf{L}$ are defined as $[\mathbf{L}]_{ij} = l_{ij}$, then the elements of its adjoint are given by $[\mathbf{L}^{*T}]_{ij} = l^*_{ji}$. Simply put, the element of the adjoint matrix $\mathbf{L}^{*T}$ is obtained by exchanging the order of the element indices in l_{ij} and taking its complex conjugate.

In a similar way we can define the adjoint kernel (Morse and Feshbach, 1954) of the integral equation in equation 4.36. Interchange the order of the data and model variables in the kernel $-2\omega^2 W(\omega)G(\mathbf{r}_g|\mathbf{r}')G(\mathbf{r}'|\mathbf{r}_s)$ and take its complex conjugate.

Specifically, multiply the adjoint kernel is $-2\omega^2 W(\omega)^*\, G(\mathbf{r}_g|\mathbf{r}')^* G(\mathbf{r}'|\mathbf{r}_s)^* = -2\omega^2 W(\omega)^* e^{ik(|\mathbf{r}'-\mathbf{r}_s|+|\mathbf{r}'-\mathbf{r}_g|)}$ $\mathbf{r}_g||\mathbf{r}'-\mathbf{r}_s|$, by the scattered data $P(\mathbf{r}_g|\mathbf{r}_s)^{scatt}$ and integrate over all data coordinates (including frequency) to give diffraction stack equation of adjoint modeling:

$$\mathbf{m} \approx \mathbf{L}^{*T}\mathbf{p} \quad = \quad \delta\mathbf{s}(\mathbf{r})^{mig},$$

or

$$\delta\mathbf{s}(\mathbf{r})^{mig} \quad = \quad \int_{data} \frac{2}{|\mathbf{r}-\mathbf{r}_s||\mathbf{r}-\mathbf{r}_g|}\{\int_{-\infty}^{\infty}[(i\omega^2)P(\mathbf{r}_g|\mathbf{r}_s)^{scatt}W(\omega)^*]e^{-i\omega(\tau_{sr}+\tau_{rg})}d\omega\}dx_g dx_s. \tag{4.46}$$

Appendix C presents the differentiation theorem which says that $(i\omega^2)P(\mathbf{r}_g|\mathbf{r}_s)^{scatt}$ Fourier transforms as the second-time derivative of $p(\mathbf{r}_g,t|\mathbf{r}_s,0)^{scatt}$, and the convolution theorem says that the product of two spectrums $(i\omega^2)P(\mathbf{r}_g|\mathbf{r}_s)^{scatt}$ and $W(\omega)^*$ Fourier transforms as their convolution $2\pi\ddot{p}(t) * w(-t)$. Thus, equation 4.46 becomes

$$\delta s(\mathbf{r})^{mig} \quad = \quad 4\pi\int_{data} \frac{[\ddot{p}(\mathbf{r}_g,t|\mathbf{r}_s,0)^{scatt} * w(-t)]_{t=\tau_{sr}+\tau_{rg}}}{(|\mathbf{r}-\mathbf{r}_s||\mathbf{r}-\mathbf{r}_g|)}dx_g dx_s. \tag{4.47}$$

Here *mig* denotes the *migration* image of the slowness perturbation, and the integration is over the planar free surface where the source and geophones are restricted to $z = 0$.

Physical Meaning. To interpret the physical meaning of equation 4.47, assume a single source at $\mathbf{r}_s$, a single receiver at $\mathbf{r}_g$, and a wideband source so that $w(t) \rightarrow \delta(t)$ and $p(t) * w(-t) \rightarrow p(t) * \delta(-t) = p(t)$. In this case, equation 4.47 becomes

$$\delta s(\mathbf{r})^{mig} = 4\pi\frac{\ddot{p}(\mathbf{r},\tau_{sr}+\tau_{rg}|\mathbf{r}_s,0)^{scatt}}{|\mathbf{r}-\mathbf{r}_s||\mathbf{r}_g-\mathbf{r}|}. \tag{4.48}$$

For 2D, the term $\tau_{sr} + \tau_{rg} = constant$ describes an ellipse in model space coordinates $\mathbf{r} = (x, z)$ with foci at the source $\mathbf{r}_s$ and receiver $\mathbf{r}_g$ points. Thus, the migration image is formed by smearing the reflection energy at time $\tau_{sr} + \tau_{rg}$ along the appropriate ellipse in $\mathbf{r}$ coordinates. For numerous traces, the migration image is formed by smearing and summing reflection energy along the appropriate ellipses in model space. The bottom illustration in Figure 4.6 shows the migration of a single trace for a zero-offset trace.

A MATLAB code for zero-offset diffraction stack migration is given below.

```
% ZERO-OFFSET ADJOINT MODELING OR
% ZERO-OFFSET DIFFRACTION STACK MIGRATION
%
for ixtrace=1:ntrace; %LOOP OVER ALL TRACES
    for ix=1:nx      %LOOP OVER ROWS OF MODEL PIXELS
    for iz=1:nz;     %LOOP OVER COLUMNS OF MODEL PIXELS
      r = sqrt((ixtrace*dx-ix*dx)^2+(iz*dx)^2);
      time = round( 1 +  r/c/dt );
      migi(ix,iz) = migi(ix,iz) + cdp3(ixtrace,time)/r;
    end;
    end;
end;
```

4.5 Summary

The Green's function is the point source impulse response of the model. In our case the model is any inhomogeneous acoustic medium where the wave motion honors the acoustic wave equation. The wave motion $\tilde{P}(\mathbf{r})$ (or corresponding inhomogeneous Green's function) in an arbitrary acoustic model is impossible to determine analytically, but $\tilde{P}(\mathbf{r})$ can be found numerically by inserting the Green's function for a homogeneous medium into Green's theorem (equation 4.24). This says that the field values within the volume are a superposition of the direct wave in the background medium and the reflections and scattering from the boundaries. These boundaries define the parts of the medium where the actual medium is not the same as the background medium. Unfortunately, the surface integral term requires knowledge of the field values that we are trying to calculate. To eliminate this stumbling block, we use the Born approximation to the Lippmann-Schwinger equation, which gives the field values as a superposition of the primary reflections from the slowness perturbations. Here, primary reflections are propagating with the background velocity, and present a good approximation to the actual seismograms if the slowness perturbations are weak, i.e., multiple scattering events are negligible. The adjoint kernel applied to the data gives the migration, the topic for the next chapter. These forward and adjoint equations under the Born approximation are the primary modeling tools and imaging in exploration geophysics.

Bibliography

[1] Barton, G., 1989, Elements of Green's functions and propagation: Oxford Science Publ., pp. 465.

[2] Bleistein, N., 1984. Mathematical methods for wave phenomena: Academic Press Inc. (Harcourt Brace Jovanovich Publishers), New York.

[3] Brebbia, C.A., 1978, The boundary element method for engineers: J. Wiley and Co., NY, NY, 189 p.

[4] Morse, P., and Feshbach, H., 1953, Methods of theoretical physics: McGraw-Hill book Co., NY, NY.

[5] Schuster, G. T., 1985. A hybrid BIE and Born series modeling scheme: Generalized Born series. J. Acoust. Soc. Am., v. 77 (3), p. 865-879.

[6] Zemanian, A., 1965, Distribution theory and transform analysis: Dover Publications, NY, NY.

4.6 Exercises

1. Prove the identity $\tilde{G}\nabla^2_{\mathbf{r}'}\tilde{P} = \tilde{P}\nabla^2_{\mathbf{r}'}\tilde{G} + \nabla_{\mathbf{r}'}\cdot(\tilde{G}\nabla_{\mathbf{r}'}\tilde{P} - \tilde{P}\nabla_{\mathbf{r}'}\tilde{G})$. Show work.

2. Show that if the Green's function for the Laplace's equation is given by

$$\nabla^2_{\mathbf{r}'}\tilde{G}(\mathbf{r}|\mathbf{r}') = \delta(\mathbf{r}-\mathbf{r}'), \tag{4.49}$$

   then the Green's theorem for Laplace's equation

$$\nabla^2_{\mathbf{r}'}P(\mathbf{r}|\mathbf{r}') = -F(\mathbf{r}), \tag{4.50}$$

   is given by equation 4.24, except now the Green function is given by equation 4.49. Show derivation in a step by step fashion, just like the Green theorem for the Helmholtz equation.

3. Compute movie of propagating harmonic wave, as described by MATLAB code below. Copy MATLAB script and run it in MATLAB. I have deliberately omitted geometrical spreading term to avoid imbalanced amplitude.

```
x=[1:300];y=[1:300];[X,Y] = meshgrid(x,y);k=.05; % Set up
                            %arrays of X and Y cooridnates
R=sqrt(X.^2+Y.^2);G=cos(k*R);imagesc(G) % Compute Green
                                        % Function for k=1;
polarity=1; % Causal Green function if polarity=1; Acausal
                            %Green Function if polarity=-1
for j=1:100;
G=cos(k*R-polarity*j*.1);imagesc(G) % Compute Movie of
                          %Propagating Wave as time increases
title([' Green Function t = ',num2str(j*.01)]); colorbar
xlabel('X (m)');
ylabel('Y (m)');
pause(.01)
end
```

Look at movie and script, and try to understand script. For example, type help meshgrid to understand how meshgrid works. What is the period of this harmonic wave? What is the wavelength? What is propagation velocity? What is apparent velocity in x direction? What is apparent velocity in y direction. Change polarity to polarity=-1. Which way is wave propagating, outgoing or incoming to the origin?

4. The Helmholtz equation for a spherically symmetric Green's function is given by

$$\nabla^2_{\mathbf{r}} G + k^2 G \;\; = \;\; \frac{1}{r^2}\frac{\partial}{\partial r}(r^2 \frac{\partial G}{\partial r}) + k^2 G = 0 \quad (for\ r \neq 0). \tag{4.51}$$

Note that if the source point $\mathbf{r}' = 0$ is at the origin then $\tilde{G}(\mathbf{r}|\mathbf{r}') = e^{ikr}/r$ where $r = |\mathbf{r} - \mathbf{r}'| = |\mathbf{r}|$. Show that the Green's function for either an outgoing (equation 4.18) or incoming wave satisfies this equation as long as $r \neq 0$.

5. Recall the volume integral in spherical coordinates over a sphere of radius R is given by

$$\int_0^R \int_0^\pi \int_0^{2\pi} r^2 dr\ sin\theta d\theta d\phi \;\; = \;\; 4/3\pi R^3. \tag{4.52}$$

Prove this. Also prove that the surface integral area is equal to the following:

$$\int_0^\pi \int_0^{2\pi} R^2\ sin\theta d\theta d\phi \;\; = \;\; 4\pi R^2. \tag{4.53}$$

Here $d\Omega = sin\theta\ d\phi d\theta$ is the differential of the solid angle, with the identity $\int d\Omega = 4\pi$.

6. A previous problem asked to show that the Green's function satisfied the Helmholtz equation when $r \neq 0$. Now you will show (Morse and Feshbach, 1953) that integrating equation 4.17 over a small sphere that surrounds the source point $\mathbf{r}' = 0$ centered at the origin yields

$$\int_{volume} (\nabla^2_{\mathbf{r}'} + k^2)\tilde{G}(\mathbf{r}'|\mathbf{r})\ r^2 dr\ sin\theta d\theta d\phi \;\; = \;\; \int_{volume} \delta(\mathbf{r} - \mathbf{r}') dx^3 = 1. \tag{4.54}$$

The integration is in the observer space. Proving that the RHS becomes 1 is obvious, by definition of the delta function. The LHS can be shown to be equal to 1 by using the following argument. Assume the integration is about a small spherical surface with radius ϵ. In this case, the volume integration over the k^2-like term in equation 4.55 becomes

$$\begin{aligned} |k^2 \int_{volume} \tilde{G} r^2 dr d\Omega| &= |k^2/4\pi \int_{volume} e^{ikr} r dr d\Omega|, \\ &\leq k^2/4\pi \int_{volume} r dr d\Omega, \\ &= k^2\epsilon^2/2, \end{aligned} \tag{4.55}$$

which goes to zero as the volume radius $\epsilon \to 0$. The inequality follows from the Schwartz's theorem, which says $\int f(x)dx \leq max(|f(x)|) \int dx$.

The only remaining thing to do is to show that the integration of the Laplacian $\nabla^2_{\mathbf{r}'} G$ goes to 1. This can be shown by using Gauss's theorem: $\int_{volume} \nabla^2_{\mathbf{r}'} \tilde{G}\ r^2 dr\ d\Omega = \int_{surface} \partial\tilde{G}/\partial r r^2 d\Omega$, plugging in the Green's function $G = -(4\pi)^{-1} e^{ikr}$ and letting ϵ go to zero. Do this. (Hint: $\partial(1/r)/\partial r = -1/r^2$).

7. Convert the zero-offset forward modeling code into a prestack modeling code where the source and receiver positions are on the free surface but are not coincident. Demonstrate the effectiveness of this code by creating shot gathers for two earth models: a point scatterer model and a single reflector interface model. A shot gather is a collection of traces where the events are excited by a common source.

Appendix A: Causal and Acausal Green's Functions

Causal Green's Functions. Applying the inverse Fourier transform

$$\mathcal{F}\cdot \;=\; \int_{-\infty}^{\infty} d\omega\ e^{i\omega(t-t_s)} \cdot, \tag{56}$$

to equation 4.18 gives the causal Green's function

$$\begin{aligned} g_c(\mathbf{r}, t - t_s|\mathbf{r}', 0) \;= \mathcal{F}(\tilde{G}(\mathbf{r}|\mathbf{r}')) = \; & -\frac{1}{4\pi} \int_{-\infty}^{\infty} e^{-i\omega(|\mathbf{r}'-\mathbf{r}|/c-(t-t_s))}/|\mathbf{r}-\mathbf{r}'| d\omega, \\ = \; & -\frac{1}{2}\delta(t - t_s - |\mathbf{r}' - \mathbf{r}|/c)/|\mathbf{r} - \mathbf{r}'|, \end{aligned} \tag{57}$$

where

$$\delta(t - t_s - |\mathbf{r}' - \mathbf{r}|/c) = \begin{cases} 1 & \text{if } t - t_s = |\mathbf{r}' - \mathbf{r}|/c, \\ 0 & \text{if } t - t_s \neq |\mathbf{r}' - \mathbf{r}|/c. \end{cases} \tag{58}$$

More precisely, $\delta(t)$ is infinite at $t = 0$ and is a generalized *delta functional* which can be only defined in terms of an inner product with a sufficiently regular function (Zemanian, 1965). With this understanding, we symbolically denote its value to be 1 for $t = 0$.

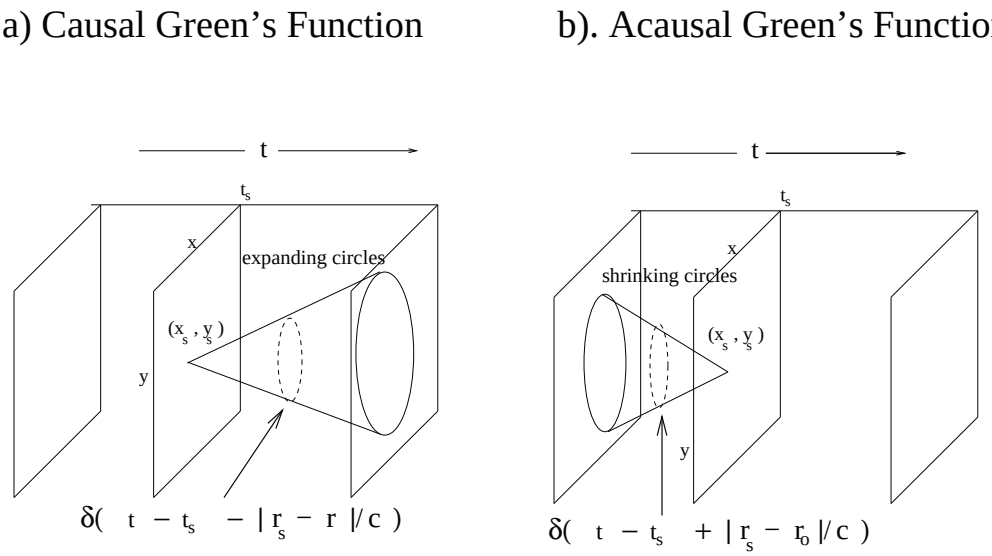

Figure 8: (a). Causal and (b). acausal Green's function in $x - y - t$ space.

Equation 58 describes an expanding circle centered about the source point; and the initiation time of the impulsive source is at time t_s and the observation time is denoted by t. The radius of the expanding circle is equal to $c(t - t_s)$ as long as the $t > t_s$. Equation 57 is a causal Green's function because the wave is not observed until it has propagated from the source point to the observation point in the *retarded time* given by $|\mathbf{r}' - \mathbf{r}|/c$. Figure 8a shows the causal Green's function expanding as a "light cone" in $x - y - t$ space.

It is easy to see that the the Green's function for a homogeneous medium is stationary so that $g_c(\mathbf{r}, t|\mathbf{r}', t_s) = g_c(\mathbf{r}, t - t_s|\mathbf{r}', 0)$. This says that the observed field depends on the time difference between the source initiation time and the observation time, no matter when the source was initiated. Thus, the shot gather obtained at noon should look like the shot gather obtained at midnight, except for a delay time of 12 hours.

The stationarity property is also true for any acoustic medium (Morse and Feshbach, 1953). A simple proof is given by multiplying equation 4.17 by a phase shift term $e^{i\omega\tau_0}$. The RHS term now is $\delta(\mathbf{r}' - \mathbf{r})e^{i\omega\tau_0}$, which is equivalent to delaying the source initiation time by the delay time τ_0. But the linearity of the LHS PDE says that the solution $G(\mathbf{r}'|\mathbf{r})e^{i\omega\tau_0}$ is the same Green's function as before, except for the time delay of τ_0. Note $G(\mathbf{r}'|\mathbf{r})e^{i\omega\tau_0}$ would not be a solution if the PDE was non-linear with terms, e.g., such as $G(\mathbf{r}'|\mathbf{r})^2$.

Acausal Green's Function. Equation 57 describes a causal Green's in a homogeneous

medium where the wavefield is *only* observed after the source initiation time τ_s. In contrast, the *acausal* Green's function is denoted by the adjoint kernel $\tilde{G}(\mathbf{r}|\mathbf{r}')^*$, which for a homogeneous medium is given as $-\frac{1}{4\pi}e^{ik|\mathbf{r}-\mathbf{r}'|/c}/|\mathbf{r}-\mathbf{r}'|$.

Applying the inverse Fourier transform

$$\mathcal{F}\cdot \;=\; \int_{-\infty}^{\infty} d\omega\; e^{i\omega(t-t_s)}\cdot, \tag{59}$$

to $\tilde{G}(\mathbf{r}|\mathbf{r}')^*$ yields the time domain acausal Green's function:

$$\begin{aligned} g_a(\mathbf{r}, t-t_s|\mathbf{r}', 0) \;&= \mathcal{F}(\tilde{G}(\mathbf{r}|\mathbf{r}')^*) = \; -\frac{1}{4\pi}\int_{-\infty}^{\infty} e^{i\omega(|\mathbf{r}'-\mathbf{r}|/c+(t-t_s))}/|\mathbf{r}-\mathbf{r}'|d\omega, \\ &= \qquad\qquad -\frac{1}{2}\delta(t-t_s+|\mathbf{r}'-\mathbf{r}|/c)/|\mathbf{r}-\mathbf{r}'|, \end{aligned} \tag{60}$$

where

$$\delta(t-t_s+|\mathbf{r}'-\mathbf{r}|/c) = \begin{cases} 1 & \text{if } t_s - t = |\mathbf{r}'-\mathbf{r}|/c, \\ 0 & \text{if } t_s - t \neq |\mathbf{r}'-\mathbf{r}|/c. \end{cases} \tag{61}$$

The acausal Green's function describes a contracting circular wavefront centered at the source point and is extinguished at time t_s and later. It is acausal because it is alive and contracting (se Figure 8) prior to the source initiation time t_s, and turns off after the source turns on! This Green's function is important because it is used for seismic migration which focuses wavefronts to their place of origin, compared to the causal Green's function that is used for modeling of exploding reflectors.

Appendix B: Sommerfeld Radiation Conditions

We will show that the outgoing Green's function in equation 4.17 satisfies the Sommerfeld outgoing boundary condition at infinity (Butko, 1972):

$$\lim_{r\to\infty}(r\frac{\partial G}{\partial r} + ikrG) \;=\; 0. \tag{62}$$

Differentiating $G = e^{-ikr}/r$ with respect to r and substituting into equation 62 we get:

$$\lim_{r\to\infty}(ikre^{-ikr}/r - ikrG - G) \;=\; \lim_{r\to\infty}(ike^{-ikr} - ike^{-ikr} - e^{-ikr}/r) \to 0. \tag{63}$$

Notice that the acausal or incoming Green's function $G = e^{ikr}/r$ will not satisfy this radiation condition. The Sommerfeld boundary condition is also needed to show that the integrand of the surface integral in equation 4.24 goes to zero at infinity.

Appendix C: Fourier Identities

The foward and inverse Fourier transforms are respectively given by

$$\tilde{F}(\omega) \;=\; \frac{1}{2\pi}\int_{-\infty}^{\infty} f(t)e^{-i\omega t}dt, \tag{64}$$

$$f(t) = \int_{-\infty}^{\infty} \tilde{F}(\omega) e^{i\omega t} d\omega, \tag{65}$$

The following are Fourier identities, where the double-sided arrows indicate the functions are Fourier pairs and $\mathcal{F}$ indicates the forward Fourier transform.

1. **Differentiation:** $\partial^n/\partial t^n \longleftrightarrow (i\omega)^n$. This property is proved by differentiating equation 65 w/r to t.

2. **Convolution Theorem:** $f(t)*g(t) = \int f(\tau)g(t-\tau)d\tau \longleftrightarrow \tilde{F}(\omega)\tilde{G}(\omega)$. This property is proved by applying the Fourier transform to the convolutional equations

$$\begin{aligned} \mathcal{F}[f*g] &= \mathcal{F}[\int_{-\infty}^{\infty} f(\tau)g(t-\tau)d\tau], \\ &= \frac{1}{2\pi}\int_{-\infty}^{\infty} e^{-i\omega t}[\int_{-\infty}^{\infty} f(\tau)g(t-\tau)d\tau]dt. \end{aligned} \tag{66}$$

   Interchanging the order of integration we get

$$\mathcal{F}[f*g] = \frac{1}{2\pi}\int_{-\infty}^{\infty} f(\tau)[\int_{-\infty}^{\infty} e^{-i\omega t} g(t-\tau)dt]d\tau, \tag{67}$$

   and defining the integration variable as $t' = t - \tau$

$$= \frac{1}{2\pi}\int_{-\infty}^{\infty} f(\tau)[\int_{-\infty}^{\infty} e^{-i\omega(t'+\tau)} g(t')dt']d\tau, \tag{68}$$

   and using the definitions of the Fourier transform of $g(t)$ and $f(t)$ we get

$$= \tilde{G}(\omega)\int_{-\infty}^{\infty} f(\tau)e^{-i\omega\tau}d\tau, \tag{69}$$

$$= 2\pi\tilde{F}(\omega)\tilde{G}(\omega). \tag{70}$$

   We will often denote the convolution of two functions $f(t)*g(t)$ by the $*$ symbol.

3. **For real $f(t)$: $f(-t) \longleftrightarrow \tilde{F}(\omega)^*$:** This property is easily proven by taking the complex conjugate of equation 65 to get $f(t)^* = f(t) = \int \tilde{F}(\omega)^* e^{-i\omega t}d\omega$ and then apply the transform $t = -t'$.

4. **Correlation: $f(t)*g(-t) = f(t)\otimes g(t)$:** By definition $f(t)*g(-t) = \int f(t-\tau)g(-\tau)d\tau$. By changing the dummy integration variable $\tau \to -\tau'$ we get $f(t)*g(-t) = \int f(t+\tau')g(\tau')d\tau' = f(t)\otimes g(t)$, where $\otimes$ represents correlation.

Appendix D: Uneven sampling to Even Sampling MATLAB Code

The MATLAB code for getting an even sampled function sampled at dt from an unevenly sampled function is

```
function [even,deceven]=resmp(uneven,time,dt)
%%%%%%%%%%%%%%%%%%%%%%%%%%%%%%%%%%%%
% Resamples input series uneven(t) with argument t in seconds
% so that output series deceven(t1) is evenly sampled with dt sampling interval
% Assumes an even sampled time interval in t1;
% Crude nearest neighbor interpolation..you might try use fancier interpolator.
% uneven  - input- Uneven sampled function
% time    - input- 2-way time of each uneven value
% dt      - input- sample interval in time for resampled data
% even    -output- Even sampled function
% deceven -output- Decimated data at dt sampling rate
%%%%%%%%%%%%%%%%%%%%%%%%%%%%%%%%%%%%
nun=length(uneven);dtprime=dt;
tmin=min(time); tmax=max(time);
dt=max(diff(time))*3;
dtt=tmax-tmin;
nt=round(dtt/dt+1);
even=zeros(nt,1);istart=1;
for i=1:nun-1;   % Loop over uneven samples in time
   x1 = uneven(i); x2 = uneven(i+1);x=[x1 x2];
   t1 = time(i); t2 = time(i+1);t12= round((t2-t1)/dt+1);
   y=resample(x,t12,1);iend=round(t12/2)+1;
   even(istart:istart+iend-1)=y(1:iend);
   istart=istart+iend+1;
end
nl=length(even);ttime=[1:nl]*dt+time(1);
for i=1:nl-1;    % Kill 0 values of even
if even(i)<.1;even(i)=even(i-1);end
end
dt=dtprime;
deceven=even;
nttt=round(dtt/dt)+1;  % Decimate data if too many
if nttt<nl;
r=round(nl/nttt);
deceven=decimate(even,r);
end
subplot(311);plot(time,uneven);title('Original Velocity vs Time')
n=length(even);
subplot(312);plot(even);title('Original Velocity vs Sample Number')
n=length(deceven);t=[1:n]*dt+time(1);
subplot(313);plot(t,deceven);title('Decimated Even Sampled dt  Velocity vs Time')
```